Simple and eco-friendly thermal regeneration of granular activated carbon from the odour control system of a full-scale WWTP: Study of the process in oxidizing atmosphere

Márquez, P. [a,ϕ], Benítez, A. [b,ϕ], Hidalgo-Carrillo, J. [c], Urbano, F.J. [c], Caballero, Á. [b], Siles, J.A. [a], Martín, M.A. [a,*]

[a] Department of Inorganic Chemistry and Chemical Engineering, Area of Chemical Engineering, University of Cordoba, Campus Universitario de Rabanales, Carretera N-IV, km 396, Edificio Marie Curie, 14071 Córdoba, Spain

[b] Dpto. Química Inorgánica e Ingeniería Química, Instituto Universitario de Nanoquímica (IUNAN), Universidad de Córdoba, 14071 Córdoba, Spain

[c] Departamento de Química Orgánica, Instituto Universitario de Nanoquímica (IUNAN), Universidad de Córdoba, 14071 Córdoba, Spain

[ϕ] Márquez, P. and Benítez, A. contributed equally to the work.

* Corresponding author: iq2masam@uco.es

Abstract

Adsorption by granular activated carbon (GAC) is an efficient, reliable, and well-established technique for treating malodours in wastewater treatment plants (WWTPs).

Abbreviations: AC, activated carbon; FS, fixed solids (%); GAC, granular activated carbon; GC, gas chromatography; MS, mass spectrometry; ou_E, European odour units; P0, pristine GAC sample; P1, GAC sample from pretreatment header deodorization; P1-R4, sample P1 regenerated at 4 hours (350 ºC); P2, GAC sample from sludge dewatering deodorization; P2-R3, sample P2 regenerated at 3 hours (250 ºC); S_{BET}, specific surface area (m^2/g); S_{micro}, micropore area (m^2/g); SOC, removed specific odour concentration ($ou_E/m^3 \cdot g$ GAC); TC, total concentration of desorbed gaseous compounds (µg/g GAC); TD, thermal desorption; TGA, thermogravimetric analysis; TN_s, soluble total nitrogen (mg/g GAC); TOC, soluble total organic carbon (mg/g GAC); V_{micro}, micropore volume (cm^3/g); VOCs, volatile organic compounds; VS, volatile solids (%); V_t, total pore volume (cm^3/g); WWTPs, wastewater treatment plants; XRD, X-ray diffraction; XRF, X-ray fluorescence.

However, when the lifespan of GAC is over, it becomes a hazardous industrial waste, which is mostly discarded in landfills. In the framework of a sustainable economy, this work proposes an oxidative thermal regeneration of GAC from the odour control system of an urban WWTP for reuse, mainly as an odour adsorbent in WWTPs, avoiding the use of high-cost inert atmosphere and complex additional post-treatments. In this sense, GAC, from two deodorization points of the abovementioned facility, the pretreatment header (P1 sample) and sludge dewatering (P2 sample), has been characterized in depth, both before and after its regeneration. Previous characterization has shown that GAC regeneration conditions depend on the nature of adsorbed odorants after the same operating time, while post-regeneration characterization has proven the recovery of the GAC's original properties. Thus, specific surface area (S_{BET}) values above 550 m^2/g have been reached for both P1 and P2, considerably exceeding the pristine sample (P0) value of 406 m^2/g. Furthermore, the microporous structure was also recovered in both samples, highlighting the case of the almost non-porous P1 sample, whose micropore volume exceeded 1.27 times the value of the P0 sample (0.180 cm^3/g) after regeneration. On the basis of the above, and taking into account the good regeneration efficiencies reached (72 - 98 %), the oxidative thermal regeneration at temperatures no higher than 350 ºC can be a simple and sustainable alternative to revalue GAC used in WWTPs.

Keywords: deodorization, granular activated carbon, oxidative thermal regeneration, reuse, WWTP.

1. Introduction

Increasingly stringent environmental regulations, the recovery of high added value chemicals in industry, or the need to find new solutions for energy storage have

increased the production and use of activated carbon (AC) in recent decades [1–3]. In this context, AC is an excellent material for removing pollutants from water environments [4], for gas purification [5], or as a component of advanced energy storage systems, such as rechargeable batteries [6,7] and supercapacitors [8,9].

Traditionally, the raw materials used for ACs' production come from non-renewable and high-cost sources, such as wood, peat, lignite, coal, petroleum fractions, and derivatives, such as polymers [10,11]. Therefore, much research has been devoted to the preparation of AC using more sustainable and economic precursors, including agricultural residues (rice husk, corn straw, bagasse, etc.) and industrial or household wastes (sludge, animal waste, garden waste, etc.) [10,12]. Moreover, coconut shells, woods, and bamboo have been used to develop an alternative method of low-cost AC production [1,13]. The mentioned biomass sources allow for low-cost and sustainable ACs. However, large quantities are required to be used in energy storage systems, and in certain cases, these products may be competitive with human or animal feed. The most common example of this problem could be for the bioethanol production process, where edible products, such as corn and sugar cane, are usually used [14].

At present, AC regeneration is a way of avoiding the use of raw materials to manufacture new ACs. According to El Gamal et al. [15], several regeneration methods can be selected, depending on the nature of the pollutant, recovery cost, and process conditions. These include thermal, chemical, microwave, electrochemical, supercritical carbon dioxide, and bio-regeneration methods. Among them, thermal regeneration under inert atmosphere is the most widely used on an industrial scale, with three main indicators to evaluate the process feasibility: mass loss, adsorption capacity, and granular strength of the regenerated AC. Nevertheless, because of the conditions required for this thermal regeneration, landfill AC deposition is still considered the most

economical option, due to both the high cost of the inert gasifying agent and energy, since high operating temperatures (above 500 ºC) are required [16].

The properties of AC depend on the starting material used for its manufacture and the conditions of the regeneration process (if this is carried out). The most characteristic properties are surface area, pore size, particle size, surface chemistry, hardness, ash content, and pH (in aqueous suspensions). These properties can be modified depending on the activation and carbonization processes used to obtain AC. It is predominantly performed by a physical or chemical activation method. In addition, ACs can be subjected to various chemical treatments, such as acids and bases, that increase their pore volume, adsorption selectivity, and functional groups content [17,18]. Agricultural waste-based ACs have been treated with different chemical agents such as HCl, H_2SO_4, HNO_3, and H_3PO_4 [19–21], as well as $ZnCl_2$, KOH, and NaOH [22–24]. As a result of these activation processes, active carbons can be designed with the appropriate characteristics to retain different types of compounds on their surface, for example, acting as filters to remove gaseous pollutants [5,25].

In wastewater treatment plants (WWTPs), activated and impregnated carbons can be used independently or in combination to remove many different odour-causing compounds [26]. In this sense, granular activated carbon (GAC) packed-bed systems are widely used for deodorization in WWTPs, due to their ability to easily adsorb a wide range of odorants, such as VOCs, mercaptans, ammonia and H_2S [27]. Virgin GAC adsorbs volatile organic compounds (VOCs), but it has a relatively low capacity to adsorb inorganic H_2S, which is reported in the literature as the main malodorous compound in WWTPs [28,29]. For this reason, in order to neutralize this odorant, WWTPs typically use GAC impregnated with alkali compounds, such as NaOH or KOH. The reaction of these compounds with atmospheric CO_2 leads to the formation of

corresponding carbonates, facilitating the transfer of H_2S to the solid phase and promoting its oxidation to elemental sulphur or sulphur oxides [30,31]. According to Estrada et al. [25], a disadvantage of GAC filtration in WWTPs is that this system presents high annual packed-bed-material requirements (0.8 ± 0.6 kg/$(m^3/h)_{air\ treated}$) because of the short lifespan of GAC (approximately six months). These carbon beds could use up to a maximum of 10,000 kg of GAC [31]. When the lifespan of GAC used in deodorization is over, it becomes a hazardous industrial waste, which is mostly discarded in landfills through authorized waste managers, resulting in a significant economic and environmental cost [27]. Thus, with the objective of promoting a circular economy, international organizations have established legislation to reduce landfill waste deposition. For example, the European Parliament and Council [32] established, in its Directive 2018/850, that "Member States shall take the necessary measures to ensure that by 2035 the amount of municipal waste landfilled is reduced to 10% or less of the total amount of municipal waste generated (by weight)".

In this context, the regeneration of contaminated GAC is an attractive alternative for facilities that routinely use this adsorbent. Moreover, in a non-profit sector such as wastewater treatment (which includes the deodorization of its gaseous emissions), simple and low-cost alternatives are necessary in order to avoid the drawbacks of thermal regeneration under inert atmosphere. For this reason, a simple oxidative thermal regeneration of GAC from an urban WWTP is proposed in this work. The objective is to evaluate the abovementioned regeneration process, based on the physico-chemical, textural and structural properties of GAC. To achieve this, two GAC samples from different deodorization points at the WWTP were characterized, both before and after regeneration. Both high regeneration efficiencies and recovery of original properties of the GAC might promote its valorisation, thereby avoiding the use of raw materials to

manufacture new GACs and the accumulation of hazardous waste in landfills. In this sense, this study demonstrates, for the first time, that thermal regeneration in an air atmosphere at temperatures no higher than 350 ºC can be a sustainable alternative to revalue GAC used in WWTPs, mainly as an odour adsorbent in these facilities.

2. Materials and methods

2.1. Deodorization process and GAC samples

GAC samples were supplied by an urban WWTP located in the province of Seville, Spain. This treatment plant, based on conventional treatment with activated sludge, anaerobic digestion and mechanical dehydration of sludge, with an average daily flow of 255,000 m^3/d, serves a population equivalent of 950,000. It uses adsorption by GAC as an odour control system. In this deodorization system, the air stream is passed over a bed of adsorbent (GAC), and the odour-causing compounds are retained. In this work, the GAC samples, with the same operation time, came from two different odour sources (Scheme 1):

- P1 is a GAC sample which comes from pretreatment header deodorization. At this WWTP, pretreatment header includes roughing operations, water elevation using worm screws, and screening. It is the first step of integral wastewater treatment.
- P2 is a GAC sample which comes from sludge dewatering deodorization. Sludge from anaerobic digestion is dehydrated by centrifuges. This is one of the last steps of the abovementioned treatment, prior to sludge storage in silos.

Scheme 1. *Schematic flow diagram of the urban WWTP*.

When the adsorbent needs to be replaced, the used GAC is discarded in a landfill as hazardous waste (code: 06 13 02) [33], and it is subsequently replaced by pristine GAC, impregnated with NaOH (P0 sample). This GAC is made from coconut shell and its technical characteristics, specified by the manufacturer, are as follows: average particle diameter of 3.7 mm, iodine number (minimum) of 1000 mg/g, and 4% ash content.

2.2. Characterization of the used and regenerated GAC samples

2.2.1. Physico-chemical characterization

2.2.1.1. Elemental analysis

X-ray fluorescence (XRF) was used to analyse the elemental composition of the adsorbent materials. Spectra were acquired with a Rigaku wavelength dispersive X-ray fluorescence (WDXRF) spectrometer ZSX Primus IV. The system was equipped with a 4 kW rhodium target X-ray tube (operating at maximum voltage of 60 kV and current of 150 mA), ten analyser crystals, a flow proportional counter for light elements detection, and a scintillation counter for heavy elements.

2.2.1.2. Surface functional groups

The Boehm method [34] was used to determine the concentration of remaining surface functional groups present in the GAC samples under study. To quantify the concentration of acidic groups (in mmol per gram of adsorbent), the abovementioned samples (0.25 g each) were added to a 50 mL NaOH solution (0.1 M) and stirred for 48 h at 170 rpm and 25 ºC. After that, the suspension was filtered and three aliquots (3 mL each) of the filtrates were back titrated using 0.1 M HCl solution (in order to neutralize the excess base) and phenolphthalein as an indicator. To quantify the concentration of basic groups, the GAC samples were added to a 50 mL HCl solution (0.1 M), being

stirred under the same conditions described above. Then, the suspension was filtered, and three aliquots of the filtrates were back titrated using 0.1 M NaOH, in order to neutralize the excess acid.

2.2.1.3. Moisture, FS, VS, pH, conductivity, TOC, and TN_s

The methodology proposed by the U.S. Department of Agriculture and the U.S. Composting Council [35] was used to quantify the following variables (in triplicate): pH, conductivity (mS/cm), soluble total organic carbon (TOC, mg/g GAC), and soluble total nitrogen (TN_s, mg/g GAC), which were measured in the aqueous extract (1:25 ratio), while moisture (%), fixed solids (FS, %), and volatile solids (VS, %) were analysed in the solid fraction.

2.2.2. Textural properties

Nitrogen adsorption/desorption data were obtained at liquid nitrogen temperature (77 K) using a Micromeritics ASAP 2020 M apparatus. Pore size distribution was calculated by the density functional theory (DFT) method applied to the adsorption branch of the isotherms. The specific surface area (S_{BET}) was calculated using the Brunauer–Emmett–Teller (BET) equation in a relative pressure range of 0.04–0.20. The t-plot method was used to estimate the micropore area (S_{micro}). The total pore volume (V_t) was calculated at a relative pressure of p/p_0 = 0.98. The micropore volume (V_{micro}) was calculated according to the Dubinin-Radushkevich equation [36].

2.2.3. Structural characterization

X-ray diffraction (XRD) patterns for both pristine and regenerated samples were obtained in a Bruker D8 Discover X-ray diffractometer equipped with monochromatic Cu Kα radiation (λ = 1.5406 Å). The patterns were recorded within the 5–80° (2θ)

range, using a step size of 0.04° and 1.05 s per step. Pattern Diffraction File database was used for the identification of crystalline phases.

2.3. Olfactometric measurements

With the objective of quantifying the removed specific odour concentration (SOC, $ou_E/m^3 \cdot$g GAC) by the GAC samples, 0.5 g of each sample was introduced into 4-L Nalophan® sampling bags and maintained in isothermal conditions for 24 h. The bags were previously filled with odourless compressed air. The filling time was 30 s, and experiments were carried out at 40 ºC.

Dynamic olfactometry was the method used to quantify the odour concentration (ou_E/m^3), which is necessary to subsequently calculate the SOC. All odour concentration data are expressed in accordance with the reference conditions described in standard EN 13725 [37] (i.e. 20 ºC, 101.3 kPa on a wet basis). A TO8 olfactometer developed by Olfasense GmbH, based on the 'Yes/No' method, was used to determine the odour concentration. This variable was calculated as the geometric mean of the odour threshold values of each panellist, multiplied by a factor which depends on the olfactometer dilution step factor. The panellist group consisted of four people, each selected based on their sensitivity to the n-butanol reference gas, as described in EN 13725 [37].

2.4. Quantification of desorbed compounds

A gas chromatography/mass spectrometry (GC/MS) instrument, coupled to a thermal desorption (TD) unit, was used to quantify the VOCs retained by the GAC samples. Both H_2S and SO_2 were quantified by gas chromatography/flame photometric detector (GC/FPD). Thus, the total concentration of desorbed gaseous compounds (TC, µg/g GAC) was calculated by taking into account the two abovementioned measurements.

2.4.1. TD-GC/MS

First, 44.5 mg of each GAC sample (P0, P1, and P2) was weighed and put in individual microchambers at 40 ºC. Fifteen minutes after putting the samples in the microchambers (equilibrium time), individual, freshly cleaned adsorption tubes were inserted in the lid of each microchamber with an adjusted dynamic flow at 50 mL/min (flow coming from the emitted headspace by the sample). After 30 min (sampling time), the tubes on the lid of each microchamber were removed and inserted into the TD-GC/MS system for chromatographic analyses.

After collecting the VOCs in the adsorption tubes, they were inserted into the TD unit coupled to the GC/MS. The instrumentation system consisted of a gas chromatograph (GC; TRACE 1310, Thermo Fisher Scientific), mass spectrometer (MS; ISQ 7000, Thermo Fisher Scientific), and thermal desorption unit (Unity2-xr Markes International, UK). After being removed from the tube by thermal desorption (280–330 ºC), volatile compounds were captured in a cold trap at a low temperature (0 to 10°C) by thermoelectric cooling. Subsequently, the cold trap was heated to 300–350°C, according to a programmed and optimized temperature profile, to release all volatiles up to the inlet of the GC column through a transfer line for subsequent chromatographic separation. At the end of the GC column, once separated, the compounds reached the MS with different retention times, where they were fragmented and, subsequently, identified by the NIST 2017 spectra database.

Registered signals as (chromatographic) peaks were quantified by comparing their size (area under curve) with the obtained area of a known amount (ng) of a reference substance (Toluene-d_8), which was adsorbed (by direct injection using a syringe) in an additional clean tube. The peak produced by Toluene-d_8 is used as reference peak for

quantification of all peaks obtained in the sample analysis. This type of quantification, based on Toluene-d_8, is known as semiquantitative. As general approach, this TD-GC/MS system can detect substances from 0.01 to 1 ng. Depending on the sampling method used, these values can be equivalent to 0.1 and 0.5 µg/m^3, respectively. The relative standard deviation (RSD) of the values obtained by this method was below 10%. VOCs were identified with a certainty higher than 80%, most of them over 90%.

2.4.2. GC/FPD

To carry out this analysis, 0.5 g of each sample (P0, P1, and P2) were introduced into 4-L Nalophan® sampling bags, which were placed at 40 ºC and maintained in isothermal conditions for 24 h. The bags were previously filled with clean and filtered air. Three bags were prepared for each GAC, analysing each bag in duplicate. H_2S and SO_2 were quantified by a fully automatic isothermal GC (Chroma S) coupled to a FPD, developed by Chromatotec. This equipment is adequate for the analysis of sulphur compounds and is described by Toledo et al. [38]. Its detection limit is 7 ppb for both H_2S and SO_2.

2.5. Thermogravimetric analysis (TGA) and MS

To determine the limit temperature of the oxidative thermal regeneration process, P1 and P2 were subjected to TGA. These measurements were made using a Mettler Toledo-TGA/DSC under oxidizing atmosphere (21% O_2 and 79% N_2 flow) by heating the GAC samples from 35 to 350°C at 15 °C/min. In order to make comparisons, P0 was subjected to the same analysis, while P2 was also subjected to TGA from 35 to 250 ºC. During the thermogravimetric measurements, the TGA/DSC equipment was coupled to a VG PROLAB Benchtop QMS MS (Thermo Scientific) to detect some compounds resulting from TGA. Signals for CO_2, H_2O, and SO_2 were monitored through their MS peaks at m/z 44, 18, and 64, respectively.

2.6. Thermal regeneration process

The thermal regeneration of the used GAC was carried out in a tubular furnace (Carbolite Gero CTF, Parsons Lane, Hope Valley, UK) using an oxidizing atmosphere with an air flow of 50 mL/min. Before heating, a purge of the atmosphere was performed inside the furnace to ensure stable conditions of the oxidizing atmosphere, increasing the oxidant flow to 100 mL/min for at least 30 min. The thermal conditions used for the regeneration of the P1 sample were a temperature range from 35 to 350 ºC at 15 °C/min. However, for the P2 sample, heating was carried out from 35 to 250 ºC using the same temperature ramp. Therefore, the regeneration process was carried out for the GAC without physical or mechanical treatment (Scheme 2), in order to achieve two added advantages: (1) additional stages of pre-conditioning of the samples for their treatment are avoided, that is, less complexity of the process, and (2) the regenerated material is obtained, keeping the original format, and can be revalued for the same use without the need for post-treatments.

Scheme 2. *Overview of the analysis and regeneration process.*

2.7. Regeneration efficiency calculation

The regeneration efficiency is an important indicator of the process feasibility. This parameter was calculated according to Eq. (1):

$$\textit{Regeneration efficiency (dry basis) (\%)} = \frac{m_{GAC}\,(A.R.)}{m_{GAC}\,(B.R.) \cdot \left(\frac{100 - moisture}{100}\right)} \cdot 100 \qquad (1)$$

where m_{GAC} *(A.R.)* is the GAC mass after regeneration, m_{GAC} *(B.R.)* is the GAC mass before regeneration, and *moisture* is the GAC moisture (%) before regeneration.

3. Results and discussion

3.1. Assessment of pristine and contaminated GAC samples

3.1.1. Physico-chemical assessment

The results of the physico-chemical characterization of the GAC samples are shown in Table 1. Considering that pristine GAC (P0) was impregnated by the manufacturer with NaOH, the presence of basic surface groups in the GAC samples is logical. Table 1 shows the presence of the abovementioned groups in P0 and P2. However, P1 presents acidic groups because a high amount of acid compounds were chemically adsorbed during pretreatment header deodorization in the WWTP. Thus, these compounds have exhausted the basic surface groups of P0, reversing its basic pH of 9.61 towards an acidic pH of 4.13. A greater emission of acid compounds (especially H_2S) takes place at the pretreatment header, with respect to the other integral steps of wastewater treatment, because different circumstances coexist at the abovementioned step, such as anaerobic conditions, a high load of organic matter, and a high presence of microorganisms [39]. For the P2 sample, its pH is basic and very close to that of pristine GAC (P0). This observation is confirmed by analysing the concentration of basic surface groups. In this sense, the gaseous compounds emitted at the sludge dewatering step have been mainly retained by means of physical adsorption, and/or the adsorption capacity of P2 has not been exhausted for the same operational time.

Table 1. *Physico-chemical characterization of the GAC samples.*

With regard to conductivity values, these show a view of the number of gaseous compounds retained in GAC samples. As observed in Table 1, P1 presents a higher conductivity value than P2 because a higher number of ionic compounds has been retained in the first adsorbent. This fact suggests that the emission of sulphur-containing compounds (which have ionic character) is greater at the pretreatment header. In

addition, the high percentage of sulphur retained by P1 (15.25%, Table 2) in comparison with P2 (0.57%) reaffirms this observation. It is also important to note that ferric chloride ($FeCl_3$) is added to the wastewater line before sludge thickening, aiding phosphorus precipitation. Although, in parallel, $FeCl_3$ addition minimizes the presence of H_2S in the gas phase; $FeCl_3$ reacts with H_2S to form a precipitate of iron sulphide (Fe_2S_3), which settles in quiescent conditions [29]. Therefore, this also justifies the low sulphur content in P2.

Table 2. *Elemental composition of the GAC samples determined by XRF*.

TOC and TN_s values are shown in Table 1. Taking into account both variables, pristine GAC presents the lowest values, since this material has not been used in any odour adsorption process, and the determined concentrations are due to the composition of the P0 sample itself. Therefore, the differences in TOC and TN_s from these minimum values are due to odorants' adsorption. P2 presents lower TOC and TN_s values than P1, since P2 was used in the deodorization related to mechanical dehydration of sludge from anaerobic digestion. In this context, the reduction of biodegradable compounds in dehydrated sludge, because of the previous biomethanization as well as the reduction of microbial activity at the sludge dewatering step, reduce the typical odour emission derived from sludge treatment [40,41]. Consequently, the values of TOC and TN_s are also reduced in P2. Another highlight is the high moisture content of P2 compared to P1 and P0 (Table 1), which is due to sludge dewatering. The abovementioned fact could have limited the adsorption efficiency of P2, since higher moisture content lowers adsorption capacity [28].

Finally, regarding FS and VS, it is important to note that FS (%) values increase slightly (approximately 2–3%) in the contaminated GAC samples. This might be explained by the transformation of retained gases to solid compounds (such as elemental sulphur or

sulphur oxides), remaining fixed in the GAC matrix [31]. For this reason, VS (%) values decrease by the same percentage as FS values increase. In addition, this retention of compounds in the form of FS is connected to the increase in conductivity values observed for P1 and P2 with respect to pristine GAC.

3.1.2. Textural assessment

In addition to evaluating the physical-chemical properties of both the pristine and used GAC samples, it is essential to know the textural properties of these samples, since the active surface and porosity of the material are key parameters in the gas retention process of ACs (Table 3). Textural measurements are crucial to achieving optimal thermal conditions in the design of the regeneration treatment.

Table 3. *Textural properties of the GAC samples.*

The N_2 adsorption/desorption isotherms and pore size distributions (obtained by the DFT method) of samples P0, P1, and P2 are shown in Fig. 1, and the values of the textural properties were collected in Table 3. Fig. 1(a) shows that the shape of the isotherms is similar for P0 and P2, where adsorption occurs at low relative pressures, corresponding to the typical curve of microporous solids that belong to type I of the BDDT classification. The presence of a small hysteresis loop on the desorption curve is due to the presence of mesopores in the carbonaceous texture, providing both samples with a dual pore system. The S_{BET} values for P0 and P2 samples were 406 and 328 m^2/g, respectively. Likewise, S_{micro} was calculated using the t-plot method, providing, in both cases, similar values. However, the adsorption/desorption curves for the P1 sample, shown in Fig. 1(a), present a different profile than the previous ones, which can be associated with type IV of the BDDT classification, where an increase in the amount of absorbed gas occurs at intermediate relative pressures, characteristic of mesoporous

solids. P1 showed a low S_{BET} of 36 m^2/g with the absence of S_{micro}. This drastic decrease in the S_{BET} is indicative of the high number of gaseous compounds retained in P1 (pretreatment header). Additionally, these data reveal that the microporosity of AC plays a crucial role in this gas retention process, according to a report by Dissanayake et al. [42].

Figure 1. *N_2 adsorption/desorption isotherms (a) and pore size distribution (b) of the GAC samples.*

Regarding the pore size distribution, Fig. 1(b) shows a range of values between 1.5–4.0 nm for samples P0 and P2, indicative of the expected dual pore system. V_t for P0 and P2 was 0.229 and 0.191 cm^3/g, respectively, covering, in both cases, a high percentage of microporosity, around 76–79%. In contrast, the P1 sample did not show micropore sizes (below 2 nm), and its mesopore size distribution had values between 2–4 nm. Furthermore, the V_t for P1 declined sharply compared to P0, and the V_{micro} value decreased practically in the same proportion, confirming the relevant role of microporosity in the gas retention process from the WWTP.

3.1.3. Relationships between olfactometric and textural variables

Once the textural properties of the GAC samples were studied, it was interesting to connect the TC (µg/g GAC) and SOC ($ou_E/m^3 \cdot$g GAC) with variations in S_{BET} and V_{micro} (Fig. 2). On one hand, P1 presents the highest retention of odoriferous compounds (≈ 150 µg/g GAC), which is correlated with the greatest loss of S_{BET} (with respect to P0). Regarding P2, it retained a lower number of odorants (≈ 40 µg/g GAC), which is in connection with a lower S_{BET} loss. In this latter GAC, the quantified sulphur-containing compounds represent almost 66% of total adsorbed compounds (Table 4). In P1, the abovementioned odoriferous compounds (including H_2S) represent only 15%, while

other chemical families such as terpenes (30%), aliphatic hydrocarbons (18%), and aromatic compounds (18%) are more predominant. On the other hand, SOC, which provides an estimated view of the odour concentration emitted at the two odour sources considered, is also directly proportional to the S_{BET} loss. P1 presents a SOC approximately 2.5 times higher than that of P2. Therefore, the SOC might also be indicative of the GAC adsorption capacity loss.

Figure 2. *Relationships between variables: SOC, TC, S_{BET}, and V_{micro}.*

Table 4. *Mass concentration (%) of the odorous families identified in the contaminated GAC samples.*

Changes in V_{micro} values are also important to consider. A simple linear regression model ($R^2 = 0.9999$) has been used to directly correlate the loss of V_{micro} with the loss of S_{BET}. On this basis, the influence of TC and SOC on the variation of S_{BET} is practically the same as on the V_{micro} variation, thus, reinforcing the important role of micropores in WWTP deodorization.

Given all of the above, the systematic and correlative study of a large number of parameters related to pristine and used GAC samples provides a necessary basis for the subsequent analysis of the regeneration process when the GAC lifespan is over.

3.2. Oxidative thermal regeneration process

Both mass loss and adsorption capacity of the regenerated GAC are primary indicators to evaluate the feasibility of the thermal regeneration process [15]. In this sense, mass loss has been studied based on the regeneration limit temperature, while S_{BET} and V_{micro} have been used to determine the feasibility of using the regenerated GAC as an odour adsorbent material.

3.2.1. Assessment of the regeneration limit temperature

The limit temperature of the oxidative thermal regeneration, for the two used adsorbents, was determined based on the TGA results (Fig. 3). Initially, a limit temperature of 350 ºC was proposed for both GACs. The treatment of P1 at this temperature led to a mass loss of 25%. The abovementioned value is not too high, considering that mass losses range from 5 to 15% when GACs are thermally regenerated in an inert atmosphere [43]. Nevertheless, in the case of P2, the mass loss was above 80% at 350 ºC, making it necessary to reduce the regeneration limit temperature to 250 ºC for this GAC, leading to a mass loss value slightly lower than that of P1 (22%).

Figure 3. *Evolution of mass loss of the GAC samples with temperature during TGA under oxidizing atmosphere (21% O_2 and 79% N_2 flow).*

Due to TGA-MS coupling, it has been proven that P1 and P2 show different behaviours, with respect to P0, under the same operating conditions, that is, when the abovementioned adsorbents were subjected to temperatures up to 350 ºC (Fig. 4). On one hand, Fig. 4(a) shows a peak, which begins around 250 ºC and extends up to 350 ºC. It represents SO_2, which first comes from the oxidation of elemental sulphur and later from the decomposition of sulfuric acid strongly adsorbed in small pores [30]. These facts are the main causes of the mass loss that takes place in the regeneration of P1. Therefore, it can be said that P1 regeneration (up to a limit temperature of 350 ºC) is carried out in an appropriate manner, but treatment of the SO_2 emission will be necessary if this regeneration process is transferred to an industrial scale. For example, the exhausted gases from thermal regeneration can be collected in an absorber and converted into sulfuric acid [30]. In P1 regeneration, the combustion of adsorbed VOCs

also takes place, but it is less significant than sulphur removal. On the other hand, Fig. 4(b) shows that the combustion of P2 itself prevailed over its regeneration, due to the high CO_2 concentration detected in comparison with P0. Furthermore, an almost parallel trend of CO_2 and H_2O is observed with respect to the mass loss of P2, when this variable begins to increase significantly, because of the combustion of this adsorbent. This also justifies the need to carry out regeneration of this adsorbent at a temperature below 350 ºC (i.e. 250 ºC). It is also important to note that in P2 regeneration, the release of SO_2, with respect to P0, is insignificant. After all, this GAC has not (chemically) adsorbed H_2S because it had previously been removed by the action of $FeCl_3$. Additionally, the differences in SO_2 release between P1 and P2 during thermal regeneration are consistent with the sulphur content determined for both samples (Table 2).

Figure 4. *Results from TGA-MS coupling for P1 (a) and P2 (b) compared to P0 under oxidizing atmosphere (21% O_2 and 79% N_2 flow). C = gas concentration (ppm_v).*

3.2.2. Assessment of the adsorption capacity

Once the regeneration limit temperatures for P1 and P2 were determined (350 and 250 ºC, respectively), different regeneration times were proposed, in order to evaluate the main characteristics of the regenerated GACs, especially those that determine their adsorption capacity. As can be observed in Table 3, both regenerated carbons exceed the S_{BET} value of P0 (406 m^2/g) for all regeneration times studied (1–5 h). For these times, the regeneration efficiencies ranged between 72 - 81 % for P1, and between 91 – 98 % for P2. In addition, optimal regeneration times were established, defining themselves as those that maximize the S_{BET} of the regenerated material. The objective of establishing an optimum is because subsequent basic impregnation of the GACs

(partially or totally) would result in reduction of the surface available for physical adsorption and, therefore, the retention capacity of compounds that are adsorbed in this way, such as VOCs [29]. In this context, the optimal regeneration time was reached first for P2 (3 h), which might be due to a rapid removal of the physically adsorbed VOCs, also resulting in a better adsorption capacity of the abovementioned GAC compared to P1. In the latter case, both a higher optimal regeneration time (4 h) and limit temperature (350 ºC) were required, which could be related to the chemical adsorption (chemisorption) of H_2S that was carried out during the deodorization process at the pretreatment header, since chemisorption leads to the formation of strong bonds between adsorbate molecules (H_2S) and GAC impregnated with NaOH [31].

Finally, all gaseous pollutants have molecular diameters of less than 2 nm, which means that they are preferably adsorbed on the GAC micropores. Therefore, in order to study the possible reuse of regenerated GACs (P1 and P2) in the original process (deodorization), the V_{micro} of these materials was analysed in parallel, considering the same proposed regeneration times (1–5 h). Thus, it is observed in Table 3 that, for both P1 and P2, the V_{micro} values exceed the V_{micro} of pristine GAC (0.180 cm^3/g) for all regeneration times studied. Furthermore, the V_{micro} values are maximized for the optimal times previously considered: 0.228 cm^3/g for P1-R4 and 0.252 cm^3/g for P2-R3. Given this, it is important to highlight the result obtained in the regeneration of the almost non-porous P1 sample, recovering its original porosity, and even increasing it, through this simple and fast thermal treatment process. These results show that the regenerated GACs maintain the porous structure of pristine GAC, with a dual system of micropores and mesopores. On this basis, the granular adsorbent carbons resulting from oxidative thermal regeneration could be reused for deodorization in WWTPs. Moreover,

good regeneration efficiencies were achieved in the abovementioned thermal process, especially in the case of P2, thus demonstrating the feasibility of this technology.

3.3. Assessment of the regenerated GAC samples

Once the optimal conditions for the regeneration process were established based on the GAC mass loss and adsorption capacity, the data from the physico-chemical, structural, and compositional characterization of the regenerated materials was evaluated. In this way, it is possible to make comparisons with P0 to further explore the possibility of reusing the regenerated GACs (without the need for post-treatments), these samples being P1-R4 (P1 regenerated at 350 ºC for 4 h) and P2-R3 (P2 regenerated at 250 ºC for 3 h).

3.3.1. Physico-chemical assessment

Table 1 shows that the pH of P1-R4 is slightly higher than that of P1, which is due to the removal of acidic species because of the high temperature (350 ºC) proposed for P1 regeneration [30]. Although the pH after regeneration is higher, it does not come back to the pH of pristine GAC (9.61). Therefore, P1-R4 should be impregnated with an alkaline agent for future reuse as an odour adsorbent at the pretreatment header. The same observation can be made by taking into account the concentrations of surface functional groups. In this sense, the regeneration of P1 reduced the concentration of acidic groups, but there continues to be no evidence of the presence of basic groups (mainly required to carry out H_2S chemisorption). In the case of P2, the oxidative thermal regeneration affects pH in a similar way, obtaining a more basic pH value for P2-R3. This suggests that P2-R3 would not need to be impregnated for reuse in sludge dewatering deodorization, which represents a difference from the P1-R4 sample. This is

further confirmed by the concentrations of basic surface groups in P2-R3, which are as high as the concentrations in pristine GAC (Table 1).

Conductivity values depend on the number of gaseous compounds that have been retained in the adsorbent material. For this reason, it would be expected that the conductivity of the GAC samples would decrease after regeneration, since a thermal desorption or combustion of retained compounds is carried out. However, as observed in Table 1, the conductivity values increase for both P1-R4 and P2-R3. This might be due to the regeneration method used. According to Sabio et al. [16], high temperatures would be capable of modifying the original carbon structure, causing the transfer of certain compounds from the adsorbent composition itself to the aqueous extract, which, in turn, leads to higher conductivity values compared to unregenerated GACs. Something similar happens with the TOC value (%) in P2-R3, where a reduction after regeneration would be expected, instead of an increase. In the case of P2-R3, as mentioned above, a loss of compounds, mainly carbonaceous, occurs, which are transferred to the aqueous solution, resulting in higher TOC values compared to P2. Nevertheless, this does not happen for P1-R4, since a large number of sulphur compounds are chemically adsorbed on P1 and are strongly bound to carbon, thus, limiting the transfer of carbonaceous compounds to the aqueous extract. In this way, a reduction of the TOC value after regeneration is obtained. In terms of TN_s (%), the oxidative thermal regeneration was similarly efficient for both GACs, since the concentration of soluble nitrogen compounds was reduced to values very close to that of P0.

Table 1 also shows a decrease in moisture content (%) after regeneration, as some of the water was evaporated during the thermal regeneration process itself. Similarly, a lower

concentration of VS (%) and a slightly higher percentage of FS are also observed. Although, the variation in this respect was not very significant.

3.3.2. Structural assessment

The structural characteristics of GAC samples were analysed by XRD in Fig. 5, which shows a comparison between the XRD patterns of P0 (black line), P1-R4 (blue line), and P2-R3 (red line). P0 shows two wide and low intensity signals at ca. 26º and 43º (2θ), which are attributed to the (002) and overlapped (100) and (101) crystallographic planes of graphite (Pattern Diffraction File, PDF #41-1487). These bands demonstrate the presence of highly disordered carbons with low crystallinity, characteristics of biomass-derived carbons obtained through activation and pyrolysis processes [7,44]. According to XRF, the coconut shell AC presents, in its composition, silicon, calcium, and sodium. For this reason, other peaks of low intensity appear in the diffractogram and could be associated with minority phases, such as SiO_2 (PDF #33-1161) at 28º (2θ), CaO (PDF #37-1497), and even the usual sodium salts remaining in ACs after the synthesis process with NaOH as the activating agent [45,46].

Figure 5. *XRD patterns of pristine (P0) and regenerated GAC samples (P1-R4 and P2-R3).*

Once the regeneration process is carried out, the XRD patterns of P1-R4 and P2-R3 samples retain the main signals of P0, with slightly varying relative intensity. However, the P1-R4 regenerated sample shows several additional peaks of higher intensity, corresponding to the Na_2SO_4 phase (PDF #37-1465). The presence of this compound after regeneration must be explicated according to the oxidation of sulphides to sulphates produced during pyrolysis in an oxidizing atmosphere. AC has been confirmed as a catalyst itself for the selective oxidation of sulphide into elemental

sulphur or sulphate [47,48]. This catalytic performance is dependent on its surface chemistry and volumes of the micropores. The presence of this soluble salt (sodium sulphate) in sample P1-R4 explains the increase in conductivity of this regenerated carbon with respect to pristine GAC.

Especially noteworthy is the similarity of the diffractograms for P0 and P2-R3, demonstrating that this regenerated carbon maintains a practically unchanged crystalline structure. Thus, only a new peak is detected around 15º (2θ) and is assigned to $CaSO_4$ as a minority phase (PDF #37-1496) [46]. In this context, XRD analysis confirms that the thermal regeneration in an air atmosphere, proposed for the GAC used in WWTP deodorization, does not alter the structural properties of these ACs.

Therefore, in order to avoid both the use of raw materials to manufacture new ACs and the accumulation of hazardous waste in landfills, this work proposed a simple technology to efficiently remove odorous contamination and obtain adsorbents that might be reused. Future additional research is necessary to evaluate recovery of the VOCs emitted during the regeneration process, in order to achieve integral use of the contaminated GAC.

4. Conclusions

From the study to evaluate the GAC thermal regeneration under oxidizing atmosphere, the following conclusions can be drawn:

- The regeneration conditions for GAC depend on the nature of adsorbed compounds after the same operating time. Thus, the sludge dewatering GAC sample (P2) is representative of the physical adsorption of VOCs, requiring a limit regeneration temperature of 250 ºC and optimal regeneration time of 3 h, while the pretreatment header GAC sample (P1), which is representative of the

chemical adsorption of H_2S, requires both a higher temperature (350 ºC) and longer optimal time (4 h).

- At the optimal regeneration times mentioned above, regeneration efficiencies reached values of 94 % for P2 and 75 % for P1, thus demonstrating the feasibility of the proposed regeneration technology.
- Textural properties of the GAC are recovered and even improved after regeneration. Thus, in the optimal cases, specific surface area and micropore volume values exceeded an average of 1.45 and 1.33 times the original, respectively. Furthermore, the oxidative thermal regeneration does not alter the GAC's structural properties.
- The P1 sample needs to be impregnated with an alkaline agent after regeneration for its reuse at the pretreatment header deodorization in the WWTP, while the regenerated P2 sample can be reused in the same application without the need for post-treatments.

Given the above, thermal regeneration under oxidizing atmosphere can be a simple and sustainable alternative to revalue GAC used in WWTPs, avoiding the use of a high-cost, inert gasifying agent, the waste accumulation in landfills and the use of raw materials to manufacture new activated carbons.

Acknowledgements

This work was supported by the Spanish Ministry of Economy, Industry, and Competitiveness (MINECO), the Spanish State Research Agency (AEI) and the European Regional Development Fund (FEDER) through Projects CTM2017-88723-R and MAT2017-87541-R, and the Ministry of Education, Culture, and Sport of Spain (Grant FPU2016). The European Regional Development Fund (Project UCO-FEDER-

1262384-R) and the Chelonia Association (Mares Circulares Project) also supported the work. A. Benítez thanks the financial support from the University of Cordoba (UCO Research Plan 2019; Sub. 2.4.). Finally, the authors wish to acknowledge the technical staff from the Instituto Universitario de Nanoquímica (IUNAN) of the University of Cordoba and express their gratitude to Inmaculada Bellido and María Luisa López for their contribution to this research.

References

[1] S. Wong, N. Ngadi, I.M. Inuwa, O. Hassan, Recent advances in applications of activated carbon from biowaste for wastewater treatment: A short review, J. Clean. Prod. 175 (2018) 361–375. https://doi.org/10.1016/J.JCLEPRO.2017.12.059.

[2] M. Sevilla, R. Mokaya, Energy storage applications of activated carbons: Supercapacitors and hydrogen storage, in: Energy Environ. Sci., Royal Society of Chemistry, 2014: pp. 1250–1280. https://doi.org/10.1039/c3ee43525c.

[3] S. Román, J.M. Valente Nabais, B. Ledesma, J.F. González, C. Laginhas, M.M. Titirici, Production of low-cost adsorbents with tunable surface chemistry by conjunction of hydrothermal carbonization and activation processes, Microporous Mesoporous Mater. 165 (2013) 127–133. https://doi.org/10.1016/j.micromeso.2012.08.006.

[4] I. Ali, V.K. Gupta, Advances in water treatment by adsorption technology, Nat. Protoc. 1 (2007) 2661–2667. https://doi.org/10.1038/nprot.2006.370.

[5] X. Zhang, B. Gao, A.E. Creamer, C. Cao, Y. Li, Adsorption of VOCs onto engineered carbon materials: A review, J. Hazard. Mater. 338 (2017) 102–123.

https://doi.org/10.1016/j.jhazmat.2017.05.013.

[6] M.M. Alam, M.A. Hossain, M.D. Hossain, M.A.H. Johir, J. Hossen, M.S. Rahman, J.L. Zhou, A.T.M.K. Hasan, A.K. Karmakar, M.B. Ahmed, The Potentiality of Rice Husk-Derived Activated Carbon: From Synthesis to Application, Processes. 8 (2020) 203. https://doi.org/10.3390/pr8020203.

[7] A. Benítez, J. Morales, Á. Caballero, Pistachio Shell-Derived Carbon Activated with Phosphoric Acid: A More Efficient Procedure to Improve the Performance of Li–S Batteries, Nanomaterials. 10 (2020) 840. https://doi.org/10.3390/nano10050840.

[8] V. Subramanian, C. Luo, A.M. Stephan, K.S. Nahm, S. Thomas, B. Wei, Supercapacitors from activated carbon derived from banana fibers, J. Phys. Chem. C. 111 (2007) 7527–7531. https://doi.org/10.1021/jp067009t.

[9] H. Yang, X. Sun, H. Zhu, Y. Yu, Q. Zhu, Z. Fu, S. Ta, L. Wang, H. Zhu, Q. Zhang, Nano-porous carbon materials derived from different biomasses for high performance supercapacitors, Ceram. Int. 46 (2020) 5811–5820. https://doi.org/10.1016/j.ceramint.2019.11.031.

[10] Y. Chen, Y. Zhu, Z. Wang, Y. Li, L. Wang, L. Ding, X. Gao, Y. Ma, Y. Guo, Application studies of activated carbon derived from rice husks produced by chemical-thermal process—A review, Adv. Colloid Interface Sci. 163 (2011) 39–52. https://doi.org/10.1016/J.CIS.2011.01.006.

[11] V.K. Gupta, A. Nayak, B. Bhushan, S. Agarwal, A critical analysis on the efficiency of activated carbons from low-cost precursors for heavy metals remediation, Crit. Rev. Environ. Sci. Technol. 45 (2015) 613–668.

https://doi.org/10.1080/10643389.2013.876526.

[12] M.A. Yahya, Z. Al-Qodah, C.W.Z. Ngah, Agricultural bio-waste materials as potential sustainable precursors used for activated carbon production: A review, Renew. Sustain. Energy Rev. 46 (2015) 218–235. https://doi.org/10.1016/J.RSER.2015.02.051.

[13] P. Rajapaksha P., A. Power, S. Chandra, J. Chapman, Graphene, electrospun membranes and granular activated carbon for eliminating heavy metals, pesticides and bacteria in water and wastewater treatment processes, Analyst. 143 (2018) 5629–5645. https://doi.org/10.1039/C8AN00922H.

[14] H.B. Aditiya, T.M.I. Mahlia, W.T. Chong, H. Nur, A.H. Sebayang, Second generation bioethanol production: A critical review, Renew. Sustain. Energy Rev. 66 (2016) 631–653. https://doi.org/10.1016/j.rser.2016.07.015.

[15] M. El Gamal, H.A. Mousa, M.H. El-Naas, R. Zacharia, S. Judd, Bio-regeneration of activated carbon: A comprehensive review, Sep. Purif. Technol. 197 (2018) 345–359. https://doi.org/10.1016/j.seppur.2018.01.015.

[16] E. Sabio, E. González, J.. González, C.. González-García, A. Ramiro, J. Gañan, Thermal regeneration of activated carbon saturated with p-nitrophenol, Carbon N. Y. 42 (2004) 2285–2293. https://doi.org/10.1016/J.CARBON.2004.05.007.

[17] C.Y. Yin, M.K. Aroua, W.M.A.W. Daud, Review of modifications of activated carbon for enhancing contaminant uptakes from aqueous solutions, Sep. Purif. Technol. 52 (2007) 403–415. https://doi.org/10.1016/j.seppur.2006.06.009.

[18] Z.M. Yunus, Y. G, A. Al-Gheethi, N. Othman, R. Hamdan, N.N. Ruslan, Advanced methods for activated carbon from agriculture wastes; a

comprehensive review, Int. J. Environ. Anal. Chem. (2020) 1–25. https://doi.org/10.1080/03067319.2020.1717477.

[19] S.N. Nandeshwar, A.S. Mahakalakar, R.R. Gupta, G.Z. Kyzas, Green activated carbons from different waste materials for the removal of iron from real wastewater samples of Nag River, India, J. Mol. Liq. 216 (2016) 688–692. https://doi.org/10.1016/j.molliq.2015.12.065.

[20] Z.M. Yunus, A. Al-Gheethi, N. Othman, R. Hamdan, N.N. Ruslan, Removal of heavy metals from mining effluents in tile and electroplating industries using honeydew peel activated carbon: A microstructure and techno-economic analysis, J. Clean. Prod. 251 (2020) 119738. https://doi.org/10.1016/j.jclepro.2019.119738.

[21] J. Zhu, M. Wagner, P. Cornel, H. Chen, X. Dai, Feasibility of on-site grey-water reuse for toilet flushing in China, J. Water Reuse Desalin. 8 (2018) 1–13. https://doi.org/10.2166/wrd.2016.086.

[22] M.B. Hasan, Z.A. Hammood, Wastewater Remediation via Modified Activated Carbon: A Review, Pollution. 4 (2018) 707–723. https://doi.org/10.22059/POLL.2018.255031.430.

[23] U. Tezcan Un, F. Ates, N. Erginel, O. Ozcan, E. Oduncu, Adsorption of Disperse Orange 30 dye onto activated carbon derived from Holm Oak (Quercus Ilex) acorns: A 3k factorial design and analysis, J. Environ. Manage. 155 (2015) 89–96. https://doi.org/10.1016/j.jenvman.2015.03.004.

[24] J.F. Vivo-Vilches, E. Bailón-García, A.F. Pérez-Cadenas, F. Carrasco-Marín, F.J. Maldonado-Hódar, Tailoring the surface chemistry and porosity of activated

carbons: Evidence of reorganization and mobility of oxygenated surface groups, Carbon N. Y. 68 (2014) 520–530. https://doi.org/10.1016/j.carbon.2013.11.030.

[25] J.M. Estrada, N.J.R.B. Kraakman, R. Muñoz, R. Lebrero, A comparative analysis of odour treatment technologies in wastewater treatment plants, Environ. Sci. Technol. 45 (2011) 1100–1106. https://doi.org/10.1021/es103478j.

[26] H. Cui, S.Q. Turn, M.A. Reese, Removal of sulfur compounds from utility pipelined synthetic natural gas using modified activated carbons, Catal. Today. 139 (2009) 274–279. https://doi.org/10.1016/j.cattod.2008.03.024.

[27] P. Márquez, A. Benítez, Á. Caballero, J.A. Siles, M.A. Martín, Integral evaluation of granular activated carbon at four stages of a full-scale WWTP deodorization system, Sci. Total Environ. 754 (2021) 142237. https://doi.org/10.1016/j.scitotenv.2020.142237.

[28] R. Lebrero, L. Bouchy, R. Stuetz, R. Muñoz, Odor Assessment and Management in Wastewater Treatment Plants: A Review, Crit. Rev. Environ. Sci. Technol. 41 (2011) 915–950. https://doi.org/10.1080/10643380903300000.

[29] Water Environment Federation, Liquid Stream Fundamentals: Odor Management and Control [Fact Sheet], (2017) 1–7. https://www.wef.org/globalassets/assets-wef/direct-download-library/public/03---resources/wsec-2017-fs-028-liquid-stream-fundamentals--odor-control_final.pdf (accessed March 11, 2020).

[30] A. Bagreev, H. Rahman, T.J. Bandosz, Thermal regeneration of a spent activated carbon previously used as hydrogen sulfide adsorbent, Carbon N. Y. 39 (2001) 1319–1326. https://doi.org/10.1016/S0008-6223(00)00266-9.

[31] M.J. Martin, A. Anfruns, R. Lebrero, J.M. Estrada, C. Canals, E. Vega, Procesos

de adsorción, in: R. Muñoz, R. Lebrero, J.M. Estrada (Eds.), Caracter. y Gestión Olores En Estac. Depuradoras Aguas Residuales, Gráficas Germinal S.C.L., Valladolid (España), 2010: pp. 115–126.

[32] European Parliament and Council, Directive (EU) 2018/850 of the European Parliament and of the Council of 30 May 2018 amending Directive 1999/31/EC on the landfill of waste, Brussels, 2018.

[33] European Commission, Commission notice on technical guidance on the classification of waste (2018/C 124/01), Brussels, 2018. http://ec.europa.eu/environment/waste/hazardous_index.htm.

[34] H.P. Boehm, Some aspects of the surface chemistry of carbon blacks and other carbons, Carbon N. Y. 32 (1994) 759–769. https://doi.org/10.1016/0008-6223(94)90031-0.

[35] US Department of Agriculture and The US Composting Council, Test Methods for the Examination of Composting and Compost (TMECC), Edaphos International, Houston (TX), 2002. https://compostingcouncil.org/tmecc/ (accessed August 16, 2018).

[36] C. Nguyen, D.D. Do, The Dubinin-Radushkevich equation and the underlying microscopic adsorption description, Carbon N. Y. 39 (2001) 1327–1336. https://doi.org/10.1016/S0008-6223(00)00265-7.

[37] EN 13725, Air Quality - Determination of Odour Concentration by Dynamic Olfactometry, European Committee for Standardization, Brussels, 2003.

[38] M. Toledo, J.M. Guillot, J.A. Siles, M.A. Martín, Permeability and adsorption effects for volatile sulphur compounds in Nalophan sampling bags: Stability

influenced by storage time, Biosyst. Eng. 188 (2019) 217–228. https://doi.org/10.1016/j.biosystemseng.2019.10.023.

[39] G. Jiang, D. Melder, J. Keller, Z. Yuan, Odor emissions from domestic wastewater: A review, Crit. Rev. Environ. Sci. Technol. 47 (2017) 1581–1611. https://doi.org/10.1080/10643389.2017.1386952.

[40] T.K.L. Nguyen, H.H. Ngo, W. Guo, S.W. Chang, D.D. Nguyen, L.D. Nghiem, Y. Liu, B. Ni, F.I. Hai, Insight into greenhouse gases emissions from the two popular treatment technologies in municipal wastewater treatment processes, Sci. Total Environ. 671 (2019) 1302–1313. https://doi.org/10.1016/j.scitotenv.2019.03.386.

[41] V. Orzi, B. Scaglia, S. Lonati, C. Riva, G. Boccasile, G.L. Alborali, F. Adani, The role of biological processes in reducing both odor impact and pathogen content during mesophilic anaerobic digestion, Sci. Total Environ. 526 (2015) 116–126. https://doi.org/10.1016/j.scitotenv.2015.04.038.

[42] P.D. Dissanayake, S.W. Choi, A.D. Igalavithana, X. Yang, D.C.W. Tsang, C.H. Wang, H.W. Kua, K.B. Lee, Y.S. Ok, Sustainable gasification biochar as a high efficiency adsorbent for CO2 capture: A facile method to designer biochar fabrication, Renew. Sustain. Energy Rev. 124 (2020) 109785. https://doi.org/10.1016/j.rser.2020.109785.

[43] C.A. Chiu, K. Hristovski, S. Huling, P. Westerhoff, In-situ regeneration of saturated granular activated carbon by an iron oxide nanocatalyst, Water Res. 47 (2013) 1596–1603. https://doi.org/10.1016/j.watres.2012.12.021.

[44] A. Benítez, M. González-Tejero, Á. Caballero, J. Morales, Almond shell as a

microporous carbon source for sustainable cathodes in lithium-sulfur batteries, Materials (Basel). 11 (2018). https://doi.org/10.3390/ma11081428.

[45] T.B. Vidovix, E.F.D. Januário, R. Bergamasco, A.M.S. Vieira, Bisfenol A adsorption using a low-cost adsorbent prepared from residues of babassu coconut peels, Environ. Technol. (United Kingdom). (2019). https://doi.org/10.1080/09593330.2019.1701568.

[46] Y. Zhao, J. Dou, X. Duan, H. Chai, J. Oliveira, J. Yu, Adverse Effects of Inherent CaO in Coconut Shell-Derived Activated Carbon on Its Performance during Flue Gas Desulfurization, Environ. Sci. Technol. 54 (2020) 1973–1981. https://doi.org/10.1021/acs.est.9b06689.

[47] C. Yang, Y. Wang, H. Fan, G. de Falco, S. Yang, J. Shangguan, T.J. Bandosz, Bifunctional ZnO-MgO/activated carbon adsorbents boost H2S room temperature adsorption and catalytic oxidation, Appl. Catal. B Environ. 266 (2020) 118674. https://doi.org/10.1016/j.apcatb.2020.118674.

[48] Y. Pan, M. Chen, M. Hu, M. Tian, Y. Zhang, D. Long, Probing the room-temperature oxidative desulfurization activity of three-dimensional alkaline graphene aerogel, Appl. Catal. B Environ. 262 (2020) 118266. https://doi.org/10.1016/j.apcatb.2019.118266.

Figure 1.

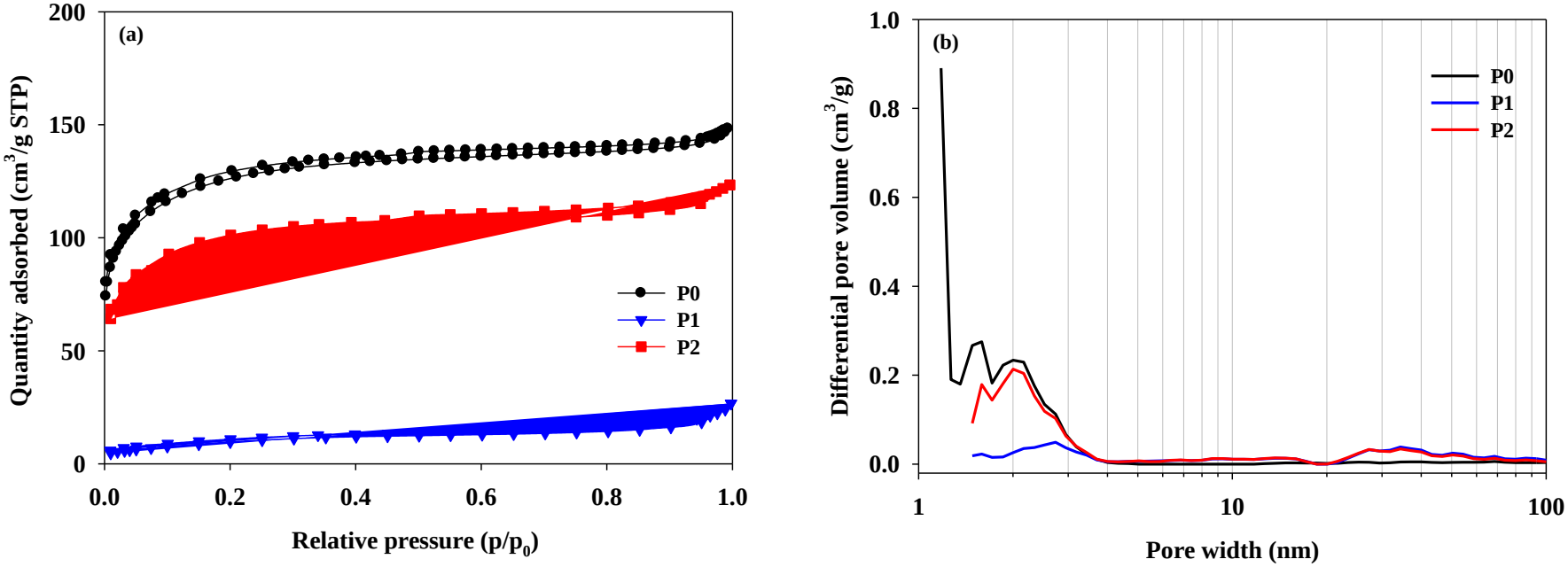
(a)
Quantity adsorbed (cm^3/g STP)
Relative pressure (p/p$_0$)
P0
P1
P2
(b)
Differential pore volume (cm^3/g)
Pore width (nm)
P0
P1
P2

Figure 2.

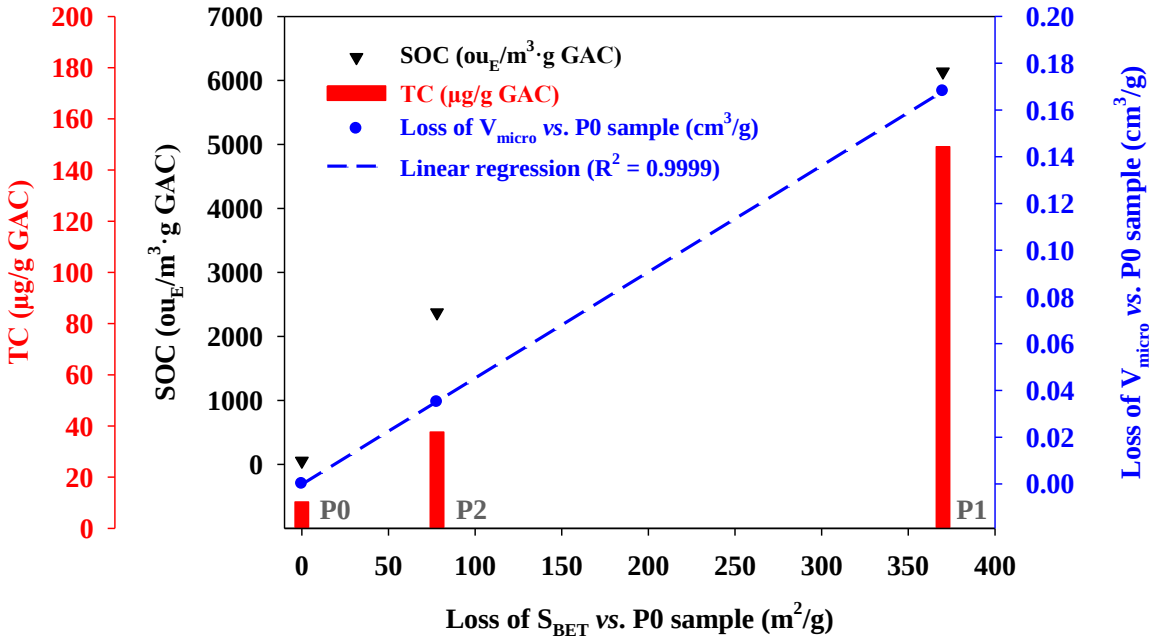
TC (µg/g GAC)
SOC (ou$_E$/m^3·g GAC)
Loss of V$_{micro}$ vs. P0 sample (cm^3/g)
SOC (ou$_E$/m^3·g GAC)
TC (µg/g GAC)
Loss of V$_{micro}$ vs. P0 sample (cm^3/g)
Linear regression (R^2 = 0.9999)
P0
P2
P1
Loss of S$_{BET}$ vs. P0 sample (m^2/g)

Figure 3.

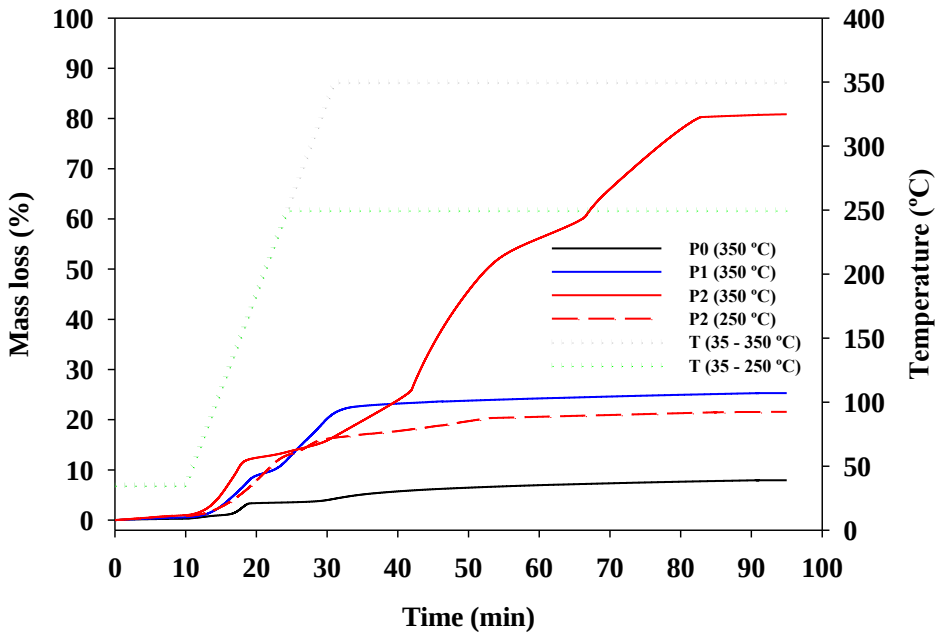
Mass loss (%)
Temperature (°C)
Time (min)
P0 (350 °C)
P1 (350 °C)
P2 (350 °C)
P2 (250 °C)
T (35 - 350 °C)
T (35 - 250 °C)
0
10
20
30
40
50
60
70
80
90
100
0
50
100
150
200
250
300
350
400

Figure 4.

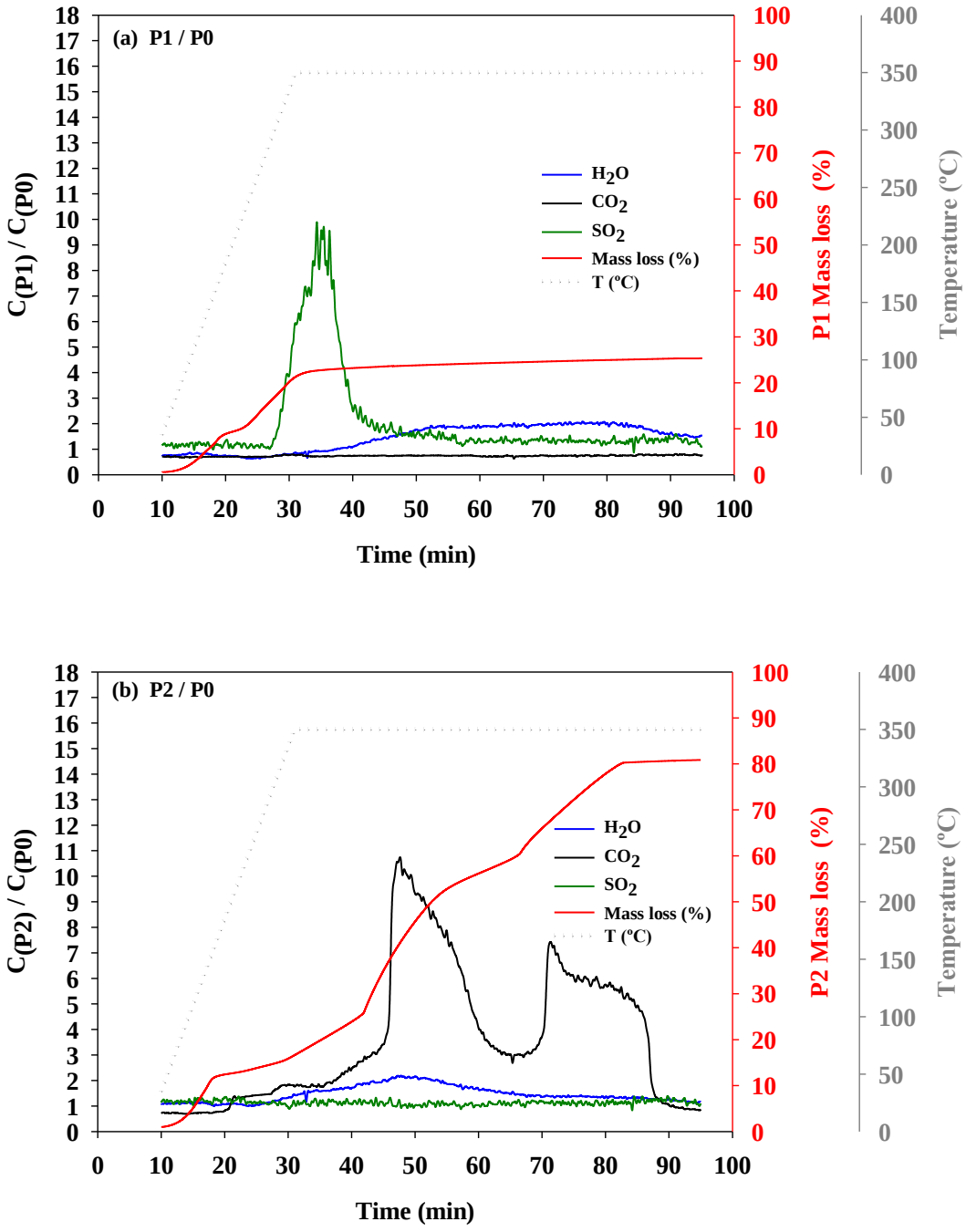
(a) P1 / P0
C(P1) / C(P0)
P1 Mass loss (%)
Temperature (°C)
Time (min)
H2O
CO2
SO2
Mass loss (%)
T (°C)
(b) P2 / P0
C(P2) / C(P0)
P2 Mass loss (%)
Temperature (°C)
Time (min)
H2O
CO2
SO2
Mass loss (%)
T (°C)

Figure 5.

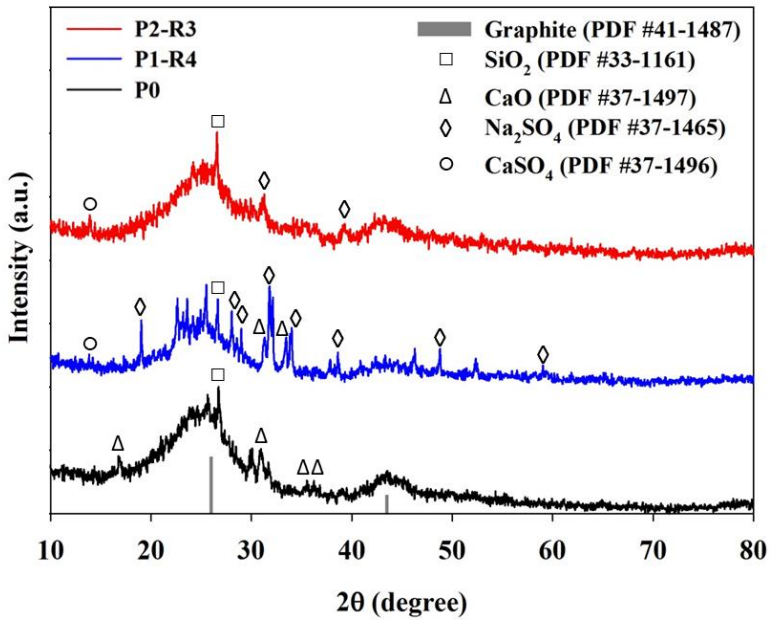
P2-R3
P1-R4
P0
Graphite (PDF #41-1487)
SiO2 (PDF #33-1161)
CaO (PDF #37-1497)
Na2SO4 (PDF #37-1465)
CaSO4 (PDF #37-1496)
Intensity (a.u.)
10
20
30
40
50
60
70
80
2θ (degree)

Scheme 1.

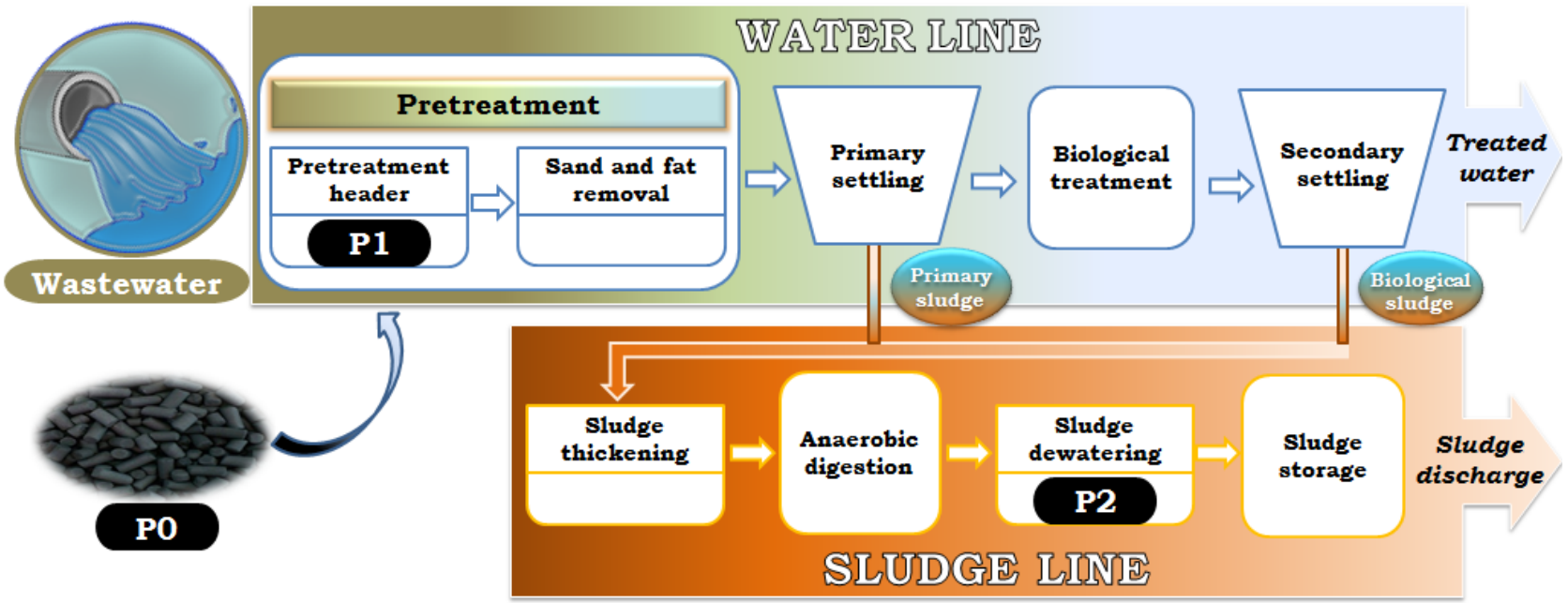
WATER LINE
Pretreatment
Pretreatment header
P1
Sand and fat removal
Primary settling
Biological treatment
Secondary settling
Treated water
Wastewater
Primary sludge
Biological sludge
P0
Sludge thickening
Anaerobic digestion
Sludge dewatering
P2
Sludge storage
Sludge discharge
SLUDGE LINE

Scheme 2.

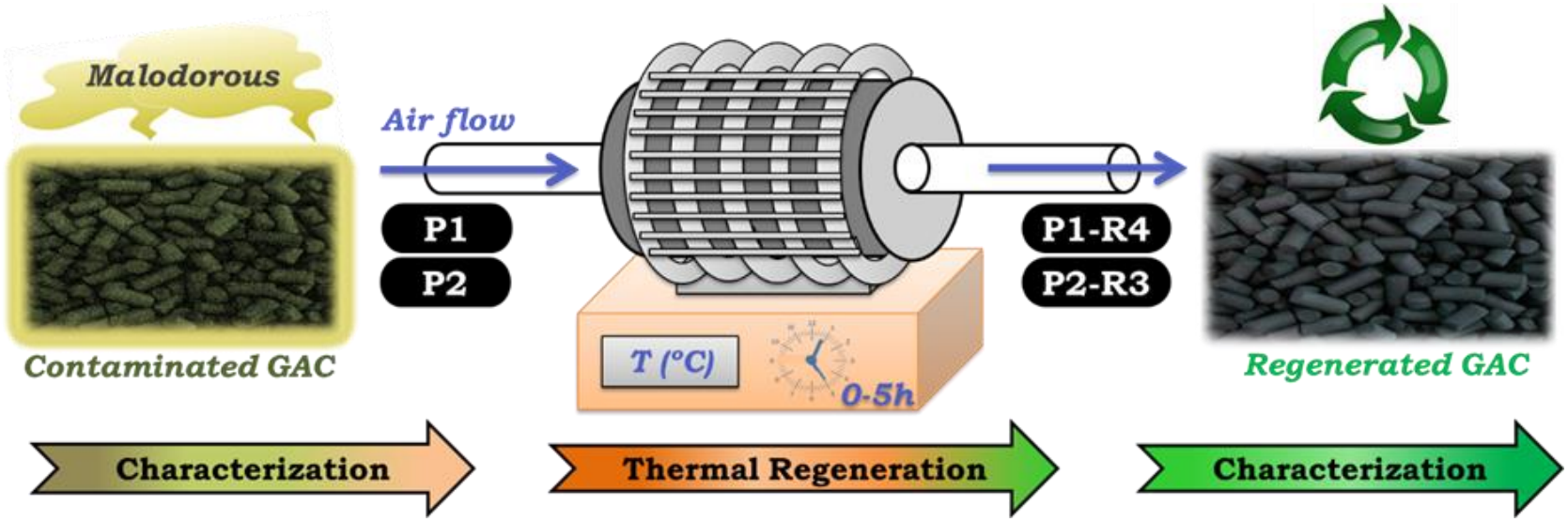
Malodorous
Contaminated GAC
Air flow
P1
P2
T (°C)
0-5h
P1-R4
P2-R3
Regenerated GAC
Characterization
Thermal Regeneration
Characterization

Table 1. *Physico-chemical characterization of the GAC samples.*

	P0	**P1**	**P1-R4**	**P2**	**P2-R3**
pH	9.61 ± 0.01	4.13 ± 0.01	4.87 ± 0.01	9.51 ± 0.01	12.43 ± 0.01
Acidic surface groups [H^+] (mmol/g GAC)	-	2.73 ± 0.38	1.05 ± 0.14	-	-
Basic surface groups [OH^-] (mmol/g GAC)	1.12 ± 0.39	-	-	1.88 ± 0.25	1.20 ± 0.25
Conductivity (mS/cm)	3.37 ± 0.01	5.85 ± 0.01	8.41 ± 0.01	4.06 ± 0.01	10.37 ± 0.01
Moisture (%)	7.20 ± 0.16	5.52 ± 0.11	3.12 ± 0.00	16.99 ± 0.00	6.17 ± 0.00
FS (%)	19.24 ± 0.18	22.35 ± 0.06	26.75 ± 0.03	21.29 ± 0.03	23.85 ± 0.15
VS (%)	80.76 ± 3.40	77.65 ± 0.17	73.25 ± 0.08	78.71 ± 0.17	76.15 ± 0.07
TOC (mg/g GAC)	0.02 ± 0.01	0.98 ± 0.01	0.61 ± 0.01	0.46 ± 0.01	3.44 ± 0.01
TN_S (mg/g GAC)	0.13 ± 0.01	0.97 ± 0.01	0.15 ± 0.01	0.23 ± 0.01	0.13 ± 0.01

FS, fixed solids; P0, pristine GAC sample; P1, GAC sample from pretreatment header deodorization; P1-R4, sample P1 regenerated at 4 hours (350 ºC); P2, GAC sample from sludge dewatering deodorization; P2-R3, sample P2 regenerated at 3 hours (250 ºC); TN_S, soluble total nitrogen; TOC, soluble total organic carbon; VS, volatile solids.

Table 2. *Elemental composition of the GAC samples determined by X-ray fluorescence*.

Elemental composition (% by weight)	**P0**	**P1**	**P1-R4**	**P2**	**P2-R3**
C	90.87 ± 0.08	78.95 ± 1.08	87.66 ± 0.17	91.55 ± 0.12	91.10 ± 0.04
Na	3.63 ± 0.02	2.79 ± 0.05	4.25 ± 0.04	3.75 ± 0.11	4.57 ± 0.18
S	2.05 ± 0.01	15.25 ± 1.02	4.66 ± 0.10	0.57 ± 0.02	0.46 ± 0.01
Si	1.14 ± 0.00	0.92 ± 0.03	1.00 ± 0.02	1.20 ± 0.01	1.06 ± 0.01
Al	0.63 ± 0.01	0.67 ± 0.01	0.77 ± 0.01	0.95 ± 0.02	0.83 ± 0.03
Ca	0.54 ± 0.00	0.57 ± 0.02	0.65 ± 0.02	0.77 ± 0.00	0.73 ± 0.01
Fe	0.50 ± 0.00	0.56 ± 0.02	0.64 ± 0.01	0.81 ± 0.02	0.73 ± 0.03
K	0.21 ± 0.02	0.05 ± 0.01	0.07 ± 0.00	0.07 ± 0.01	0.07 ± 0.00
Cl	0.20 ± 0.00	0.02 ± 0.01	0.02 ± 0.00	0.02 ± 0.00	0.03 ± 0.00
Mg	0.11 ± 0.00	0.17 ± 0.01	0.16 ± 0.01	0.17 ± 0.00	0.17 ± 0.01
Sr	0.02 ± 0.00	0.02 ± 0.00	0.02 ± 0.00	0.02 ± 0.00	0.02 ± 0.00
P	0.01 ± 0.00	0.02 ± 0.00	0.02 ± 0.00	0.03 ± 0.00	0.03 ± 0.00

P0, pristine GAC sample; P1, GAC sample from pretreatment header deodorization; P1-R4, sample P1 regenerated at 4 hours (350 ºC); P2, GAC sample from sludge dewatering deodorization; P2-R3, sample P2 regenerated at 3 hours (250 ºC).

Table 3. *Textural properties of the GAC samples.*

GAC samples	Regeneration time (h)	Regeneration efficiency (dry basis) (%)	S_{BET} (m^2/g)	S_{micro} (m^2/g)	V_t (cm^3/g)	V_{micro} (cm^3/g)
P0	-	-	406	236	0.229	0.180
P1	-	-	36	-	0.041	0.012
P1-R1	1	81.08	482	288	0.264	0.213
P1-R2	2	78.95	509	225	0.283	0.211
P1-R3	3	75.01	535	203	0.324	0.216
P1-R4	**4**	75.32	**569**	**204**	**0.347**	**0.228**
P1-R5	5	72.07	480	198	0.295	0.204
P2	-	-	328	169	0.191	0.145
P2-R1	1	98.44	467	280	0.265	0.214
P2-R2	2	94.45	497	246	0.277	0.218
P2-R3	**3**	94.53	**606**	**227**	**0.346**	**0.252**
P2-R4	4	91.96	519	181	0.293	0.214
P2-R5	5	91.53	517	172	0.294	0.212

P0, pristine GAC sample; P1, GAC sample from pretreatment header deodorization; P2, GAC sample from sludge dewatering deodorization; S_{BET}, specific surface area; S_{micro}, micropore area; V_{micro}, micropore volume; V_t, total pore volume.

Table 4*. Mass concentration (%) of the odorous families identified in the contaminated GAC samples.*

Odorous families	Mass concentration (%)	
	P1	**P2**
Terpenes	29.89	4.16
Aliphatic hydrocarbons	18.21	0.95
Aromatic compounds	17.59	24.41
Sulfur-containing compounds	15.23	65.70
Cyclic hydrocarbons	8.20	1.87
Ketones	3.99	0.24
Halogen-containing compounds	3.72	0.24
Alcohols	1.16	1.37
Aldehydes	0.65	-
Esters	0.43	0.33
Ethers	0.43	0.19
Organic acids	0.37	0.20
Nitrogen-containing compounds	0.15	-
Furans	-	0.36

P1, GAC sample from pretreatment header deodorization; P2, GAC sample from sludge dewatering deodorization.